Design, Synthesis, and Characterization of New mono, diPeptide Prodrugs, and their Bioactivity

Huda ahmed younis*
Department of Pharmaceutical Chemistry, College of Pharmacy, University of Basrah, Basrah, Iraq.
Corresponding E-mail: huda.ahmad2014@yahoo.com

Raheem Jameel Mahesein
Department of Pharmaceutical Chemistry, College of Pharmacy, University of Basrah, Basrah, Iraq.

Abstract

The synthesized two new derivatives of mono peptide H1, (Synthesis of monoPeptide (levofloxacin acid chloride with glutamine), and dipeptide H5 (Synthesis of diPeptide (The Boc-d-3,3-diphenylalanine acid chloride (Boc-d-3,3-DPAAC), using a Levofloxacin substituted. Spectroscopic data were characterized as well as reactivity indices by using techniques FT-IR, ^{1}H-NMR, and ^{13}C-NMR**.** The bioactivity was studied for two derivative compounds H1 and H5 against three types of gram-positive and three types of gram-negative Bacteria, the derivatives of levofloxacin have appeared excellent results against these Bacteria.

Keywords: mono and diPeptide, levofloxacin derivatives, glutamine and Boc-d-3,3-DPAAC.

1. Introduction

Peptides serve important biological functions despite having less structural complexity than the bigger protein molecules. A unique y-amide bond can be found in the tripeptide glutathione (y-glutamyl-L-cysteinyl glycine): It is worth remembering that the glutamic acid residue's y-carboxyl group, not the a-carboxyl group, contributes to the peptide bond. Glutathione (GSH), a substance found in almost all organisms, is essential for the transfer of amino acids, the metabolism of drugs and environmental toxins, the creation of proteins and DNA, as well as many other vital biological processes[1-3]. One category of glutathione's functions takes advantage of the antioxidant's potency as a reducing agent. Glutathione reacts with chemicals like peroxides (R-O-O-R), byproducts of O_2 metabolism, to shield cells from the damaging effects of oxidation.

Peptides have two important chemical reactions, in one of these two reactions, Peptides are hydrolyzed by boiling with a strong acid or a strong base to yield their amino acid components freely. The second reaction of the lipids is used to determine the amino acid sequence with its association with 2,4-dinitrofluorobenzene.

The available research discusses the utilization of prodrugs to get around various issues in the formulation along with managing a systemic administration, and to do a quick agent clearance of both drugs.

Many peptides' therapeutic effectiveness is further hampered by their missing prolonged half-life in systemic circulation. Polypeptides may exhibit chemical and physical instability in addition to delivery issues, making the formulation work much more difficult [4,5].

Peptide-drug conjugates (PDCs), a new type of prodrugs, are created when a particular peptide sequence is covalently joined to medication by a cleavable linker. PDCs can incorporate a significant amount of functionality: the amino acid sequence might be selected to regulate the conjugate's physicochemical properties and to enable dynamic targeting of a specific receptor on the surface of tumor cells. PDCs should not trigger unwanted immunogenic reactions because they are made from amino acids and typically carry brief peptide altitudes. Furthermore, it might also be biodegradable. Numerous distinct PDCs can be easily made thanks to various amino acid combinations. Control over the sequence permits for fine-tuning the conjugate's overall hydrophobicity and ionization. It is affecting its bioavailability in vitro and in vivo. Additionally, using straightforward HPLC procedures, PDCs' low molecular weight makes it possible to purify them for homogeneity. The molecular weight and purity of synthetic PDCs must be well controlled if the pharmacokinetics of PDCs is to be optimized [6-7]. A developing subgroup of PDCs called self-assembling PDCs aims to integrate the benefits of peptide-based prodrugs with a delivery strategy. This allows individual conjugates to build nanostructures with physicochemical features special to the pieces (Figure1) [8].

Figure 1: shows a scheme for peptide-drug conjugates containing either one drug (A) or two various medicines (B). The medicinal chemical, the carefully selected peptide, and the linker connecting the three make up every PDC. A new class of PDCs is intended to spontaneously combine from a range of well-defined nanostructures in aqueous solutions, such as nanofibers (C).

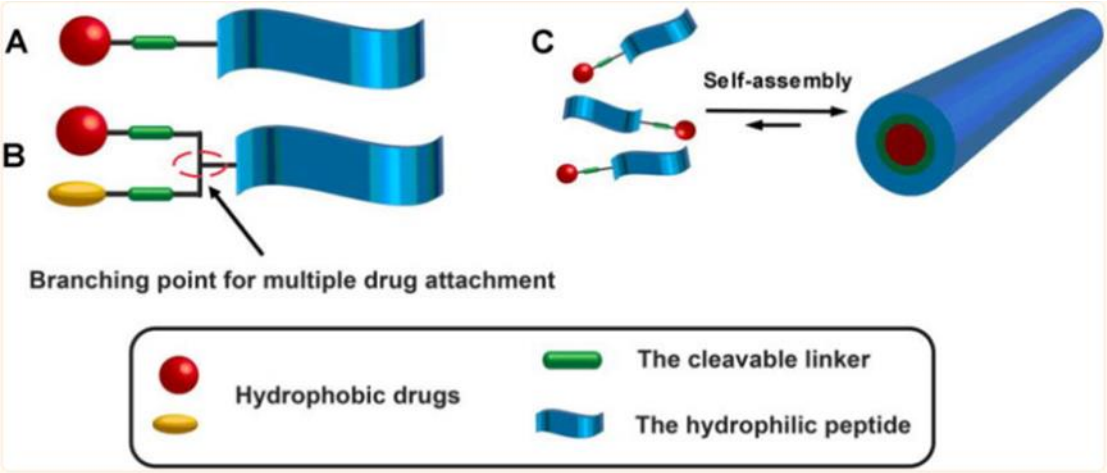

Levofloxacin A broad-spectrum fluoroquinolone antibiotic of the third generation is employed to deal with bacterial infections. The WHO's list of essential medications includes the safe and efficient medication levofloxacin. It was granted a patent in 1987 and later approved by the FDA for US medicine in 1996 [9,10].

The optical S-(-) isomer of racemic ofloxacin is the fluoroquinolone antibiotic levofloxacin. L Compared to R-(+)-ofloxacin1, it has 8 to 128 times greater activity against both gram-negative and gram-positive bacteria and maintains stereochemical stability after ingestion (i.e., it does not invert to the inactive isomer). Levofloxacin belongs to the third generation of fluoroquinolones, also known as the "respiratory quinolones," because of its

enhanced activity against gram-positive bacteria frequently associated with respiratory infections. Other quinolones in this generation include gatifloxacin and moxifloxacin (Figure 2) [11,12].

Figure 2: chemical stracture of Levofloxacin

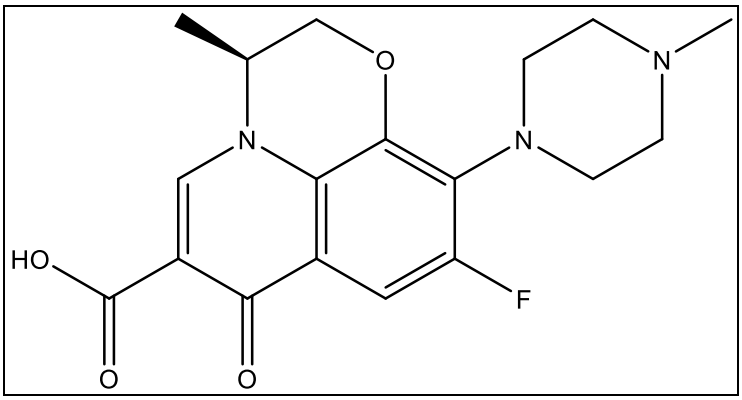

Conjugation of the peptide with levofloxacin: design and synthesis. Short peptides were attached to LVX on the carboxyl group of the tobramycin-fluoroquinolone hybrid scaffold using solid-phase peptide synthesis (SPPS). This was done to determine whether the aliphatic hydrocarbon linker and tobramycin fragment were necessary (scheme1)[13].

Since it only had one accessible reactive carboxyl group, LVX was a suitable fluoroquinolone for SPPS circumstances. However, it is understood that fluoroquinolones' carboxyl group is necessary to block their intracellular targets for DNA/DNA gyrase and topoisomerase IV. As a result, we anticipate that our covalent attachment of peptides will reduce antibacterial activity, which is essential for an adjuvant's function to prevent selective pressure that could result in the selection of resistance. In further studies, peptides will be added to fluoroquinolones somewhere else than the carboxyl group in order to study the adjuvant effect. With the help of SPPS and 4-methyl benzhydryl amine (MBHA) Rink amide resin, three series of peptide-levofloxacin conjugates, as shown in (scheme 1), were created [14, 15].

All peptide-levofloxacin conjugates have an amidated C-terminus as a result of the use of this resin. Each series consisted of conjugates with lengths ranging from one to four amino acids, the sole difference being the number of amino acids. L-diaminobutyric acid (Dab)-based short polybasic peptides were added to LVX to produce series A, where conjugates 1-4 included progressively more Dab up to four residues. The protonatable primary amine side chains are present in the polybasic peptides because this functional group is essential for increasing the permeability of the outer membrane. 20 Notably, there are five primary amines in tobramycin altogether. In order to construct a conjugate that may permeabilize the bacterial outer membrane, the ideal number of protonatable amine groups must be present. This allows us to investigate if the tobramycin carbohydrate structure was necessary. Series B was created by conjugating 5-8 of one to four L-glutamic acid (Glu) to LVX in order to control series A. Because Glu has the same number of ethylene carbon atoms in its side chain as Dab, it was chosen to study the effects of adding amino acids with different side chains, either basic or acidic functional groups. At physiological pH, the basic Dab and the acidic Glu would both contribute a general

cationic and anionic charge. The tobramycin-fluoroquinolone hybrids' conjugates 9–12 of series C, which had twelve carbons separating the polybasic peptide of series A–long tether (C12), further demonstrated that the optimal molecular linker length for the adjuvant characteristics was C12 [16-20].

Scheme 1: Levofloxacin-peptide conjugates are being researched. Series (A), constituted of Dabn-LVX, Series (B), Glun-LVX, Series (C), and Dabn-C12-LVX, were the 3 cohorts that were prepared.

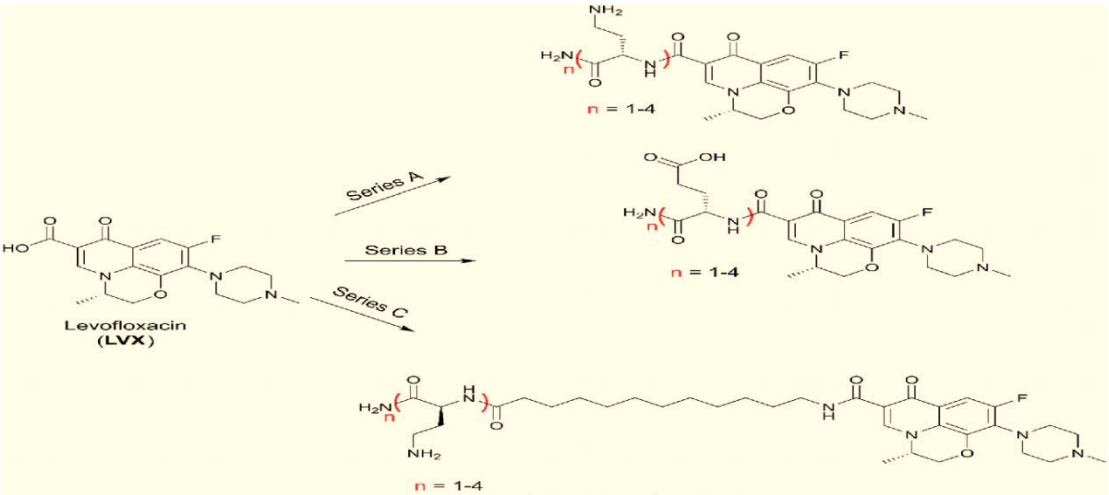

Number amino acids (n)	Series A (Dab)$_n$-LVX	Series B (Glu)$_n$-LVX	Series C (Dab)$_n$-C12-LVX
1	1	5	9
2	2	6	10
3	3	7	11
4	4	8	12

2. Experimental Section

2.1. Synthesisof monoPeptide (levofloxacin acid chloride with glutamine)

Mixed levofloxacin acid chloride (0.37gm,1mmol) and (0.146gm,1mmol) of glutamine in a dry flask containing the two compounds mixed, then 20ml of DMF was added; at room temperature, vigorous stirring for more than 24 hours was done, the combination was diffused in a clean petri dish. After the evaporation of the solvent, the bleaching repeatedly with 20 mL volumes of Acetone of the residue was applied before being accumulated. Scheme (2) depicts the Synthesis General Scheme for the Synthesis.

Scheme 2: The Compound H1 Synthesis General Scheme

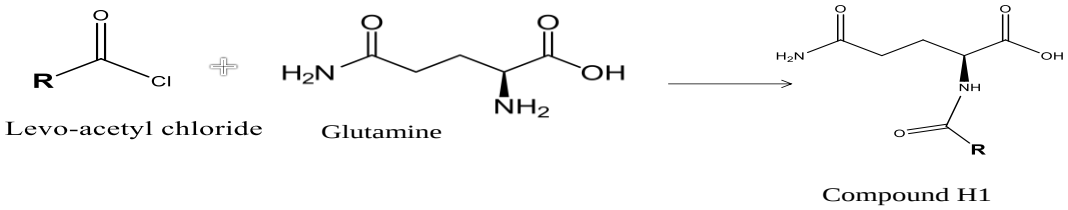

From the reaction of levofloxacin acid chloride respectively with glutamine to synthesizing the compounds H1, This suggested mechanism involves the nucleophilic strike of amino acid nitrogen lone pair on the levofloxacinoyl chloride carbonyl group carbon atom. It is

stated as the first step. The following step is chloride ion elimination. The scheme of levofloxacinoyl chloride with amino acid mechanism reaction is exhibited in Scheme (3).

Scheme 3: The combination of LAC and amino acid suggested a mechanism reaction.

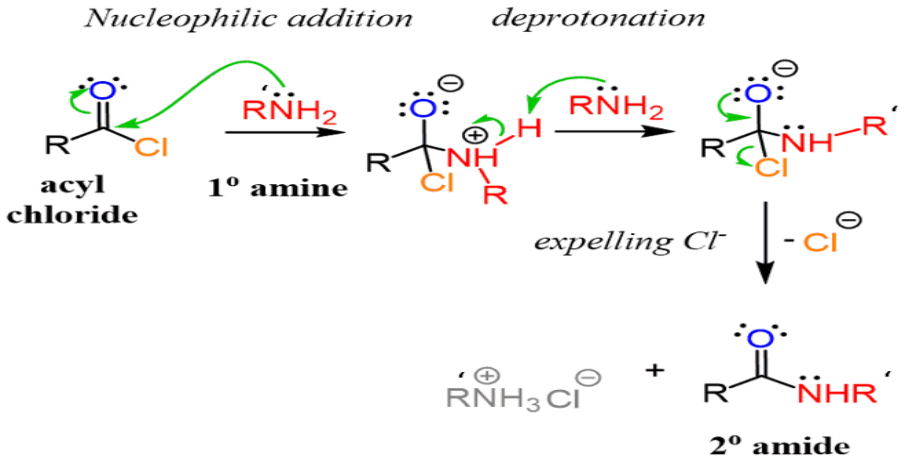

2.2. Synthesisof diPeptide (The Boc-d-3,3-diphenylalanine acid chloride (Boc-d-3,3-DPAAC)

Boc-d-3,3-diphenylalanine (2gm, 5.87 mmol) was diluted in dry dimethylformamide in a two-necked shaped flask (250 mL) (15 mL). Drop by drop adding of thionyl chloride (2 mL, 27.5 mmol) over 45 minutes of blending in an ice bath at (-5 °C), then refluxed with % hours constant stirring, and the HCl gas evolution can be studied (when the color of litmus paper is reddish). The mixture was again purified, and the deep orange-reddish water vapor condenses appeared; the precipitates were then emulsified in dry dimethylformamide (25 mL), and after that excess thionyl chloride was eliminated by doing re-filtering multiple times. The deep orange-reddish powder (1.6 g, 4.44 mmol); melting point (210 °C) was procured. The Synthesis General Scheme is displayed in Scheme (4) and Figure (2).

Scheme4: General scheme for the synthesis of Boc-d-3,3DPAAC (H5)

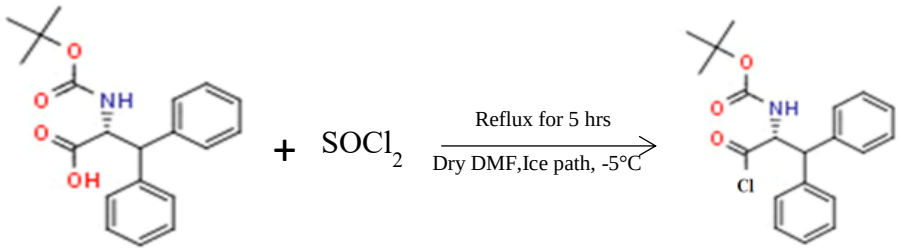

Boc-d-3,3-diphenylalanine

Boc-d-3,3DPAAC

Compound H5 is produced when boc-d-3,3-diphenylalanine and boc-glycine react with $SOCl_2$ to form acid chloride of this compound then these products react with phenylalanine then deprotected by TFA and the final product reacts with LAC to form dipeptide compounds .

The general structure of levofloxacin derivative products is depicted in Figure (2).

Figure 2: The Derivatives of Levofloxacin H1and H5 general structure

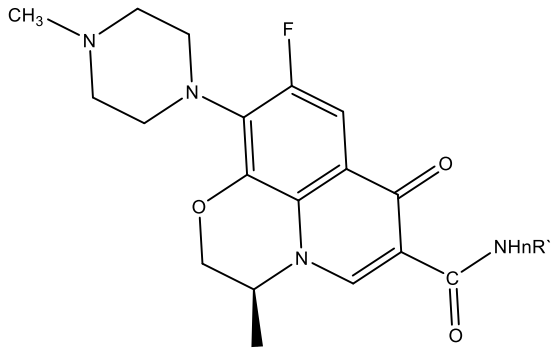

Figure 3: stracture of Boc-d-3,3DPAAC (H5)

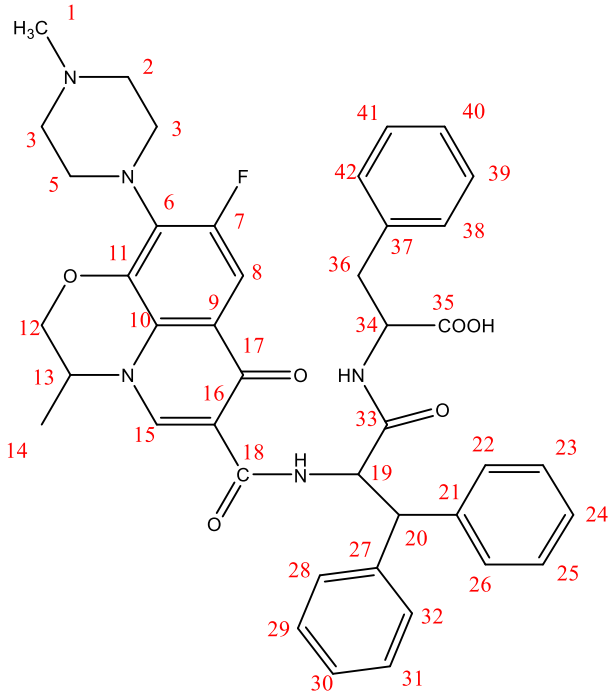

2.2.1. Instrumentation.

The infrared spectra were recorded Using potassium bromide disks on a Pye Unicam SP-3-500 infrared spectrophotometer/ SHIMAZU/Japan. 1H-NMR spectra were run at 500 MHz, on a Varian Mercury VX-500/ (INOVA/Switzerland) DMSO-d, the NMR spectrometer using TMS as an internal standard in deuterated dimethylsulphoxide. The

microanalytical data were measured in the Central Lab of College of Education for Pure Sciences, Basrah University, Iraq; also All the chemical reactions were monitored, and The melting points were measured [21].

2.2.2. Materials:

Moxalactam or cefoperazone, protects amino acid, amino acids, DCC, thionyl chloride, solvent, and mineral acids.

All materials were supplied from different companies: Schar-Lab/Spain, BIOSYNTH Carbosynth/USA, Riedel-de-Hane/ Germany, Sigma-Aldrich/Germany, Carl Roth/Germany, Santacruz Biotechnology/USA, and GLS SYSTEMS/ India.

2.2.3. Computations:

Computations were performed using Gaussian 16 revision A.03 package [18] and/or Spartan'16 parallel QC program (Wavefunction, Inc., USA). Optimized structures and spectroscopic data were obtained within DFT by employing the widely used wB97X-D/6-31G (d,p) model. Long-range corrected hybrid density functional, the wB97X-D functional [22] , includes empirical damped atom-atom dispersion corrections. wB97X-D is significantly more accurate than the commonly used functional B3LYP. Harmonic vibrational frequencies of the optimized geometries were calculated with the same model in order to verify that they are true minima (with zero imaginary frequencies). Tight SCFconvergence (energy change 1.0e−08 au) and larger integrationgrids are used. (e list of the convergence criteria followed is 5e−9 for RMS density change, 1e−7 for maximum density change, 5e−7 for direct inversion in the iterative subspace)DIES) error convergence, and 1e−5 for orbital gradient convergence. Finally, we used successfully a less-expensive computational model wB97X-D/6-31G (d) without any change in the trends obtained from the basis set 6-31G(d,p).

3. Results and Discussion

3.1. The spectrum of infrared [23, 24]

All the newly produced derivative compounds H1 and H5 have FT-IR spectra that share similarities in certain fingerprint-like bands and other bands. The essential functional group vibration bands are presented in Table (1), and the corresponding compound IR spectra are displayed in Figures(4 and 5). All the predicted bands for normal Levofloxacin, as well as the bonded amino acids glutamine, are present in all FT-IR spectra of levofloxacin derivatives. Levofloxacin derivatives H1 and H5 often have IR spectra that are very similar to those of regular Levofloxacin. It indicates that condensation between levofloxacin and amino acids took place at the chlorine-containing region of typical levofloxacinoyl chloride.

The carbonyl bond of the amide group stretching is attributed to a sturdy band between 1745 and 1685 cm^{-1} in the FT-Infrared spectra of all the newly produced compounds H1 and H5. Those are in harmony with earlier works and denote the entire condensation of levofloxacin with the study's glutamine, the carboxylic groups bond of O-H linked to the amino acid residues is accountable for levofloxacin variants 1 and 5 IR spectra, performing a robust and broad extending band vibration in the range of 3441-3286 cm^{-1}. Furthermore, the N-H bond of a secondary amide can be assigned a medium band in the range of 3258-3124 cm^{-1}.

The levofloxacin derivative compounds H1 and H5 of IR spectra show a negative band at a range of 3041-3024 cm^{-1} because of aromatic straining C-H, as well as 3 powerful bands to moderate ones at the range of 977-619 cm^{-1} because of the bending of C-H bond aromatic. A weak band was observed at the range of 2978-2823 cm^{-1} due to asymmetrical straining of aliphatic C-H bands, whereas a moderate band emerged at the range of 1423-1305 cm^{-1}

for the bending of aliphatic C-H bond, Show in figure (4 and5).

Aromatic (C=C) asymmetrical and symmetrical stretching could be associated with two prominent bands that popped up in the 1544-1455 cm^{-1} and 1479-1431 cm^{-1} ranges, and between.

Further to that, the compounds H1 and H5 of FT-IR spectra illustrate a strong band that is attributed to v(C-N) at the range of 1257-1201 cm^{-1} and assigned to (C-O) at the range of 1138-1124 cm^{-1}.

Table (1): Infrared novel levofloxacin derivatives' selected bands in the cm^{-1} unit

	ν_{aro}(C-H) Bending	**ν(C-O)**	**ν(C-N)**	**ν_{ali}(C-H) Bending**	**ν_{as}(C=C) ν_s (C=C)**	**ν(C=O) amide**	**ν_{as} (C-H) ν_s (C-H) Aliphatic**	**ν(C-H) Aromatic**	**ν(N-H) Amide**	**ν(O-H)**
H1	977 s 806 s 709 s	1126 s	1257 s	1354 s	1516 s 1479s	1712 s	2962 w	3041 s	3358 w	3441
H5	879 s 705 s 619 s	1132 s	1201 s	1305 s	1529 s 1479 s	1708 s	2978 w	3024	-	3425 br

aro=aromatic, ali=aliphatic, as=asymmetrical, s=symmetrical, s= sharp, w=weak, br=broad

Figure(4): The Compound H1 of FT-Infrared Spectrum

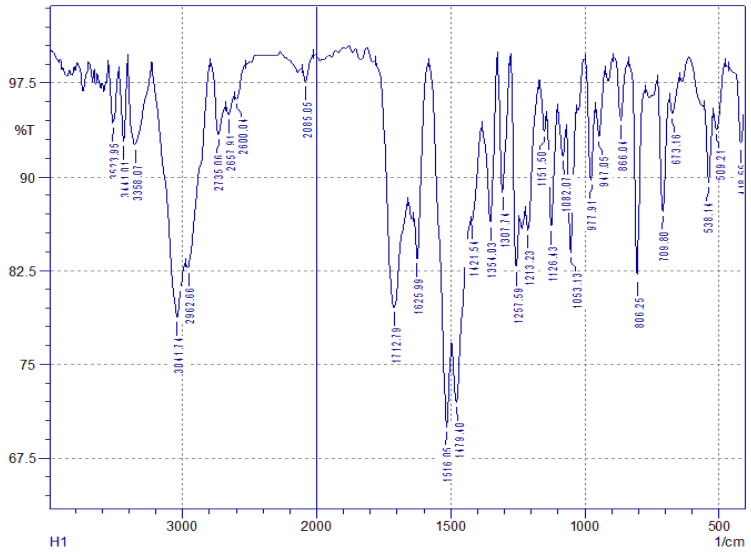

Figure(5): The Compound H5 of FT-Infrared Spectrum

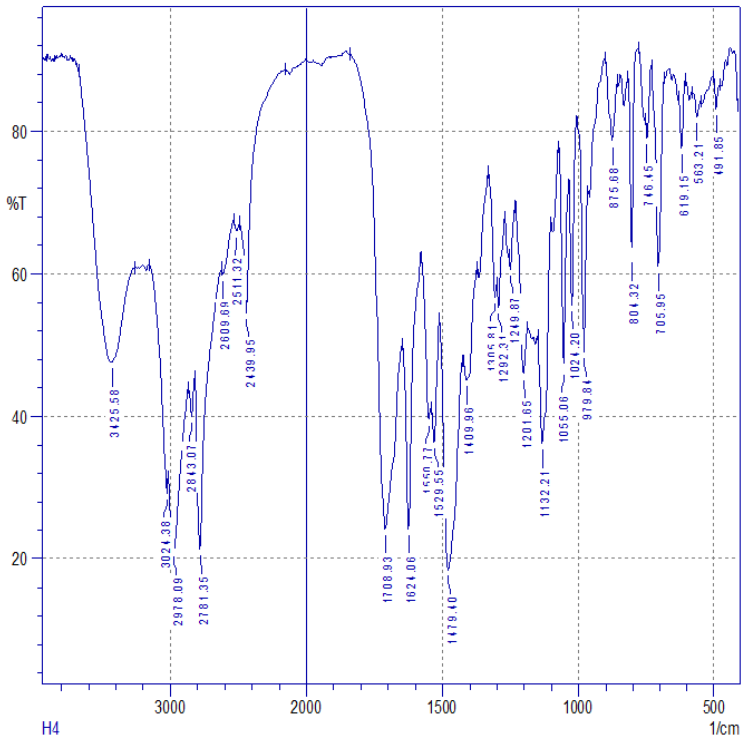

3.2. The Spectra of 1H–NMR [25]

In the DMSO-d6 solvent, the compound H1 and H5 of 1H NMR spectra were restricted. Figures (6 and 7) Typically, the fitted intensity ratio of the observed compound 1H NMR spectra depicts the expected signals. Table data (2) provides a breakdown of all levofloxacin derivatives H1 and H5, 1H–NMR.

Figure 6: The Spectrum of Compound H1 of the ^{1}H NMR

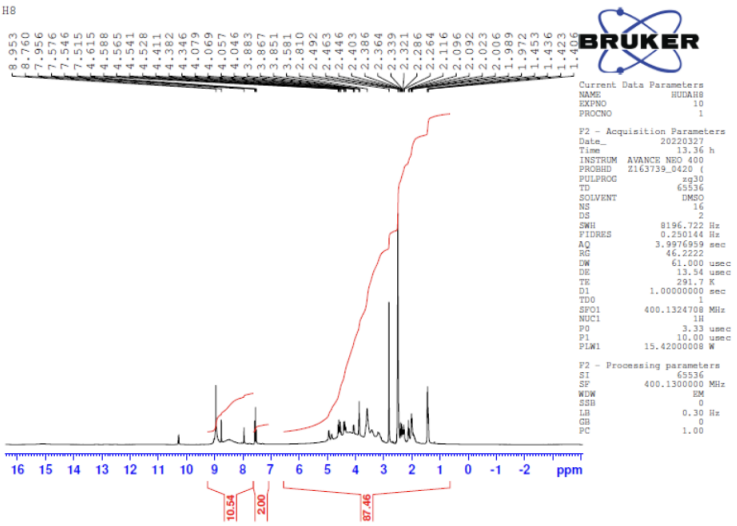

Figure 7: The Spectrum of Compound H5 of the ^{1}H NMR

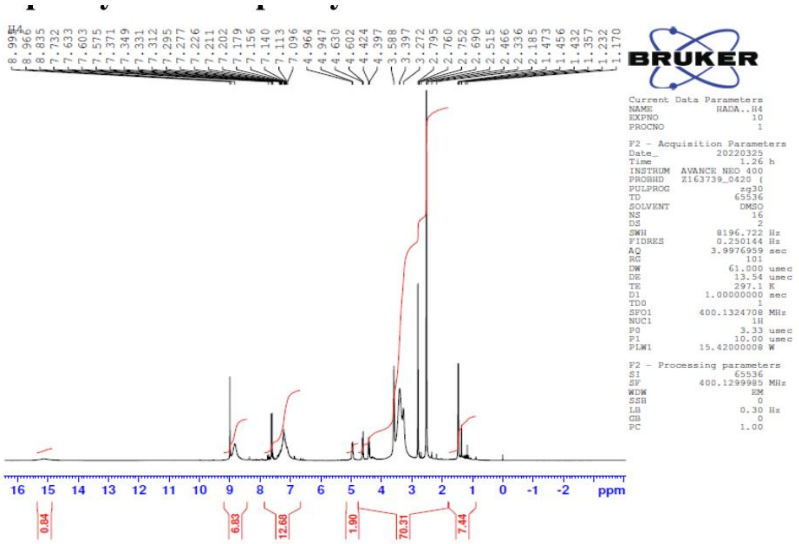

The 1H NMR spectra of the compounds, shown in the Figures above, provided additional proof that Levofloxacin completely condensed with glutamine, and phenylalanine (the amino acids) to form a -CO=NH-R (N-substitution amide) group. Table (2) clearly illustrates a broad singlet sign caused by an amide proton at 7.56 to 15.2 ppm. Additionally, all the compound H1 and H5, 1H–NMR spectra were recorded in all the anticipated levofloxacin and amino acid concentrations that were used in this work. These numbers match the information that was previously reported [26].

The aromatic protons of the phenyl group and the phenylalanine of the phenyl group can all be attributed to the various signals in the 1H NMR spectra of compounds H1 and H5 (shown in Fig.(6 and 7) which range in frequency from 7.273 to 8.99 ppm 179. Further to that, those show a single sign that can be attributed to groups of proton methyl (e.g., no.14) centered at about 1.40 ppm. Aliphatic Proton possessed

by no.2 and no.3 piperidine cyclic groups can be attributed to two triplet signals between 2.73 and 2.824 ppm, whereas the same cycle group's no.4 and no.5 can be assigned to the other two triplet signs around 3.35 and 3.88 ppm.

The aliphatic cycle proton of CH_2-O, or no.12, produces a di sign ranging from 4.046 to 4.51 ppm. The proton of carboxylic groups in amino acids, on the other hand, could be the source of the singlet sign during strong chemical shifts (weak field) in the 9.2-15.11 ppm range.

Table (2): The ^{1}H NMR data

Compound	Type of proton	Chemical shift in ppm	Desecription
H1	CH_3	1.406 (d) 2.116 (s)	(3H), Protons of CH3 group at position 14 (3H), Protons of (N-CH3) group at position 1
	CH_2	2.096 (d) 2.264 (d) 2.810 (t) 3.88 (t) 4.046 (d)	(2H), Protons of CH2 groups at position 21 (2H), Protons of CH2 groups at position 22 (2H), Protons of CH2 groups at position 2,3 (2H), Protons of CH2 groups at position 3,4 (2H), Protons of CH2 groups at position 12
	CH	3.531 (bc) 4.615 (m) 7.953 (S)	(1H), Protons of CH groups at position 13 (1H), Protons of CH groups at position 19 (1H), Protons of CH groups at position 8
	H	8.953 (s)	(1H), Protons link C groups at position 15
	OH	10.3 (S)	(1H), Protons of COOH group position 20
	NH NH_2	8.76 (s) 7.576 (S)	(1H), Protons of NH group (2H), Protons of NNH2 group
H5	CH_3	1.473(d) 2.515(s)	(3H), Protons of CH3 group at position 14 (3H), Protons of (N-CH3) group at position 1
	CH_2	2.795(t) 3.272(d) 3.397(t) 4.397(d)	(2H), Protons of CH2 groups at position 2,3 (2H), Protons of CH2 groups at position 36 (2H), Protons of CH2 groups at position 3,4 (2H), Protons of CH2 groups at position 12
	CH	3.585(bc) 4.424(q) 4.63(d) 4.964(t) 7.732(s) 7.226-7.633	1H), Protons of CH groups at position 13 (1H), Protons of CH groups at position 34 (1H), Protons of CH groups at position 20 (1H), Protons of CH groups at position 19 (1H), Protons of CH groups at position 8 (1H), Protons of CH groups at position 22,23,24,25,26,28,29,30,31,32,38,39,40,41,42
	H	8.99(s)	(1H), Protons link C groups at position 15
	OH	15.11	(1H), Protons of COOH group
	NH	8.35-8.96	(1H), Protons OF two NH group

- S is singlet, d is doublet, t is triplet, q is quartet, m is multiplet,br is broad signal

The DMSO-d6 solvent was employed to record the ^{13}C NMR spectra of levofloxacin derivatives H1 through H5. Figures (8 and 9) portrayed the ^{13}C NMR spectra of generated compounds H1 through H5, while Table (3) comprised the ^{13}C NMR data. Further confirmation of the properties of the developed molecule emerged from ^{13}C-NMR spectra [26].

Figure 8: Compound Spectrum H1 ^{13}C NMR

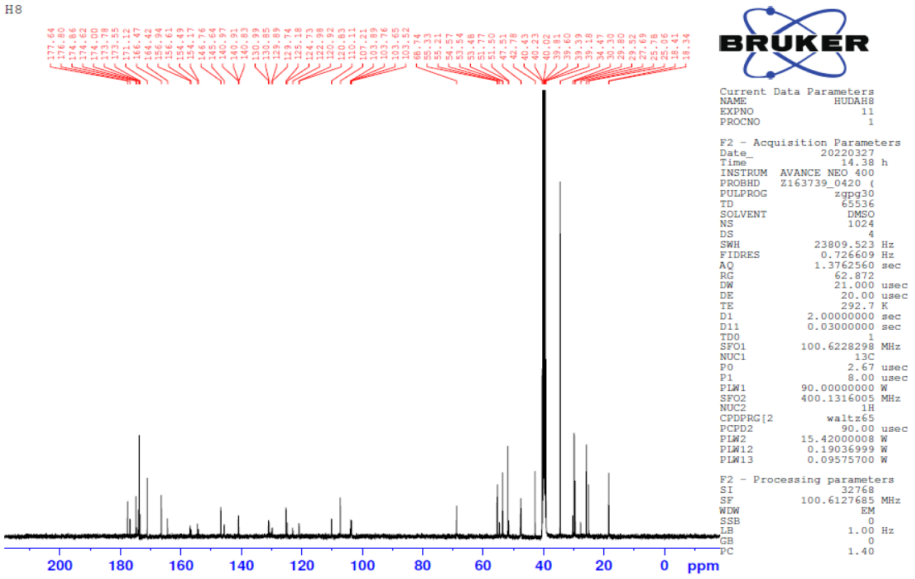

Figure 9: Spectrum of ^{13}C NMR of the compound H5

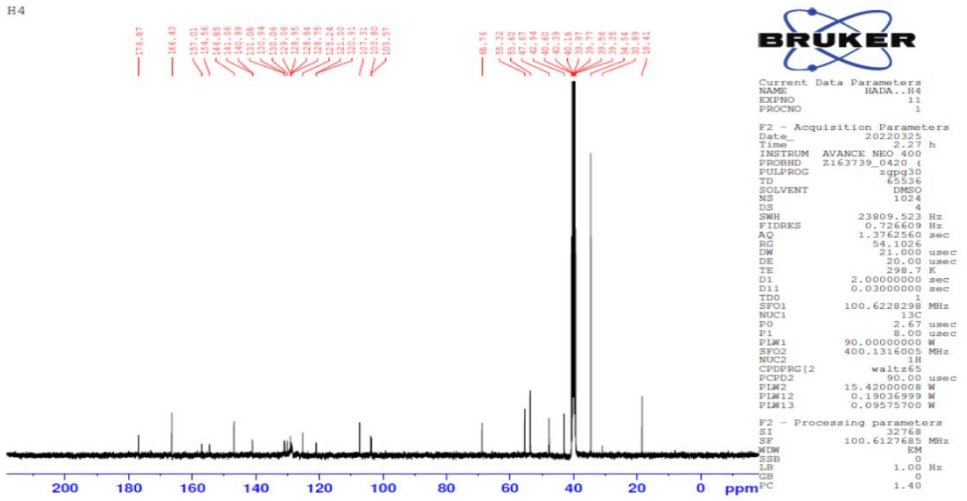

Table (3): The ^{13}C-NMR data of all products

Compound	chemical shift (δ) in (ppm)	Description of carbon environment
H1	18.41	Carbon environment at position 14
	34.47	Carbon environment at position 21
	39.6	Carbon environment at position 22
	42.78	Carbon environment at position 1
	47.5	Carbon environment at position 2,3
	53.46	Carbon environment at position 4,5
	53.54	Carbon environment at position 19
	55.33	Carbon environment at position 13
	68.7	Carbon environment at position 12
	103.89	Carbon environment at position 8
	107.21	Carbon environment at position 16
	120.83	Carbon environment at position 9
	125.18	Carbon environment at position 10
	130.99	Carbon environment at position 6
	140.91	Carbon environment at position 11
	146.76	Carbon environment at position 15
	154.49	Carbon environment at position 7
	166.42	Carbon environment at position 18
	174.62	Carbon environment at position 23
	176.8	Carbon environment at position 17
	177.64	Carbon environment at position 20
H5	18.41	Carbon environment at position 14
	34.54	Carbon environment at position 36
	39,97	Carbon environment at position 20
	42.94	Carbon environment at position 1
	47.67	Carbon environment at position 2,3
	53.6	Carbon environment at position 4,5,19,34
	55.2	Carbon environment at position 13
	68.76	Carbon environment at position 12
	103.57	Carbon environment at position 8
	107.31	Carbon environment at position 16
	120.91	Carbon environment at position 9
	125.24	Carbon environment at position 10
	128-130.06	Carbon environment at position 22,23,24,25,26,28,29,30,31,32,38,39,40,41,42
	130.94	Carbon environment at position 6
	131.08	Carbon environment at position 37
	140.99	Carbon environment at position 11
	141.06	Carbon environment at position 21,27
	146.65	Carbon environment at position 15
	154.56	Carbon environment at position 7
	157.01	Carbon environment at position 33
	166.43	Carbon environment at position 18
	176.87	Carbon environment at position 17,35

4. Bioactivity

Antibiotic susceptibility experimental findings revealed that various bacteria had taken different approaches to the tested drugs. At (250 mg / L) & (400 mg / L), most bacteria isolated in gram-positive and gram-negative demonstrated strict sensitivity to the generated compounds (H1 and H5).

The results of Figures (10 to 15) demonstrate that the monopeptide (H1) antibiotic is more efficacious against streptococcus and Staphylococcus at a concentration of 250 mg/L.

These antibacterial peptides are described as a type of natural microbicide that is especially harmful to bacterial cells while barely toxic to mammalian cells. They function by drawing negatively charged bacterial cells with a reasonably high electrostatic force. These peptides are categorized according to their content, amino acid sequences, and secondary structures.

Despite the absence of an outer membrane or LPS in Gram-positive bacteria, these organisms have a highly anionic structure that makes them a good target for cationic antimicrobial peptides. Cationic antimicrobial peptides are more effective against Staphylococcus strains in which the acid of teichoic has already been transformed, culminating in an improved anionic charge. The antimicrobial peptide is thought to replace the cations customarily dealt with by LPS in Gram-negative bacteria.

Gram-negative bacteria have LPS (Lipopoly Saccharid) structures in their cell walls, with the hydrocarbon chains providing low fluidity to the LPS minor area. In blocking the flow of chemicals like antibiotics, the outer membranes are efficient [27].

The porin channels are frequently used by bacteria with considerable outer membrane components to enter the cell. In general, gram-negative bacteria's Porin channels allow access to hydrophilic substances [28].

Our results demonstrate that (H1) Samples at (100mg/L, 200mg/L) Concentration levels are less efficient against bacteria of gram-positive and bacteria of gram-negative. On the other hand, at (50 mg/ L), all the samples (H1 and H5) show the lowest inhibition on the various tested bacteria. Low layer-by-layer permeability of the outer membrane to lipophilic Solutions is the cause of this resistance to antibiotics [29].

Drug Synergy is also considered to be a solid clinical notion because it allows for lower drug concentrations than are normally used, resulting in fewer adverse effects while proving the medication's efficacy [30]. It has been investigated how the dipeptide antibiotic promotes the growth of bacteria. The prepared Samples (H5) that were utilized the most were very efficient against E. coli at 250 and 400 mg/L. Even though pseudomonas exhibited a lesser inhibition of the growth of bacteria in all the doses of an antibiotic (All are shown in figures 10 and 11.

The two least effective of bacterial mechanisms involved in intrinsic resistance have been decreased outer sheath permeability (the LPS (lipopolysaccharide) in gram-negative bacteria was most prominently) and the biological activity of the efflux pump.

Furthermore, plasmid is an important element of the genetic structure of pseudomonas some of them can confer antibiotic resistance and other compounds of bacterial [31].

To create combinatorial medicines that minimize patient toxicity while maximizing treatment success, the significant synergy and antagonism effects are frequently explored at optimal intermediate medication doses [32]. The level of inhibition present in each sample varying depending on the organism. There might be a diversity of different Zone Sizes preseasons, like the maturity and the quantity of inoculate that is injected into the solid medium, the incubation conditions, the medium composition, and changing receptors on the bacterial cells' surface. Eventually, these peptides are thought to be expansive microbicides [33,34].

Figure 10: H1 antibacterial activity against by the reference strain of Streptococcus A. Levofloxacin 250 micrograms/ml was used to treat the bacterial strain B. C, bacterial strain given a 50 microgram/ml treatment. D, bacterial strain given a 100 microgram/ml treatment. E, a bacterial species that received 200 g/ml of treatment. F, 400 microgram/ml-treated strain of bacteria

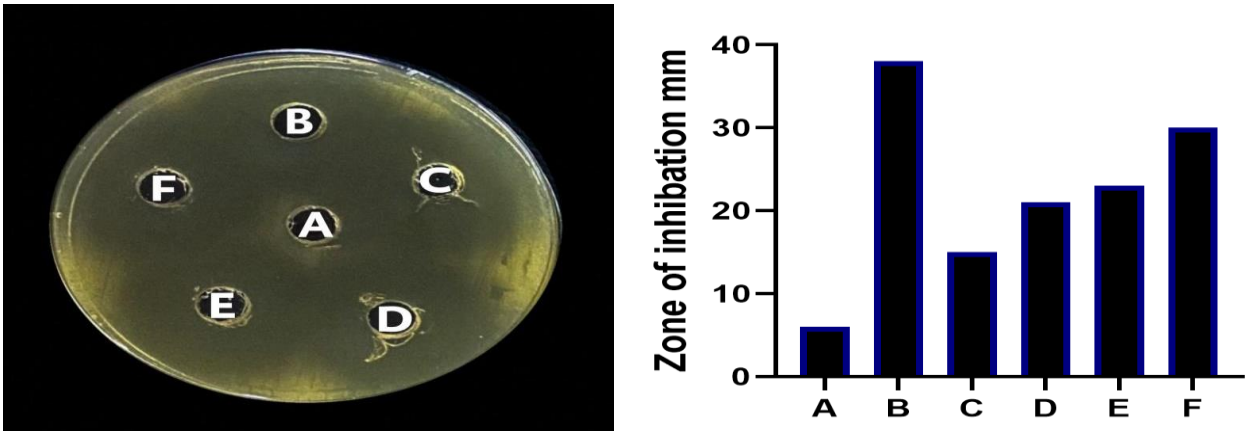

Figure 11: H1 antibacterial action on pseudomonas. A, command. Levofloxacin 250 micrograms/ml was used to treat the bacterial strain B. C, bacterial strain given a 50 microgram/ml treatment. D, bacterial strain given a 100 microgram/ml treatment. E, a bacterial strain that received 200 g/ml of treatment. F, 400 microgram/ml-treated strain of bacteria.

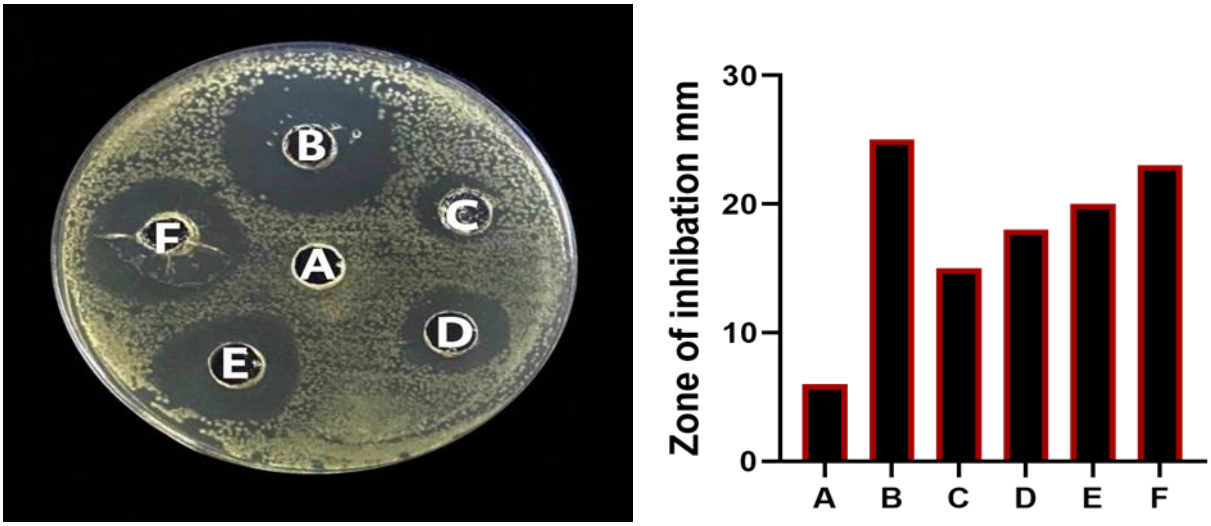

Figure 12: H1 antibacterial ability to combat Staphylococcus bacteria. A, command. Levofloxacin 250 micrograms/ml was used to treat the bacterial strain B. C, bacterial strain given a 50 microgram/ml treatment. D, bacterial strain given a 100 microgram/ml treatment. E, a bacterial strain that received 200 g/ml of treatment. F, 400 microgram/ml-treated strain of bacteria

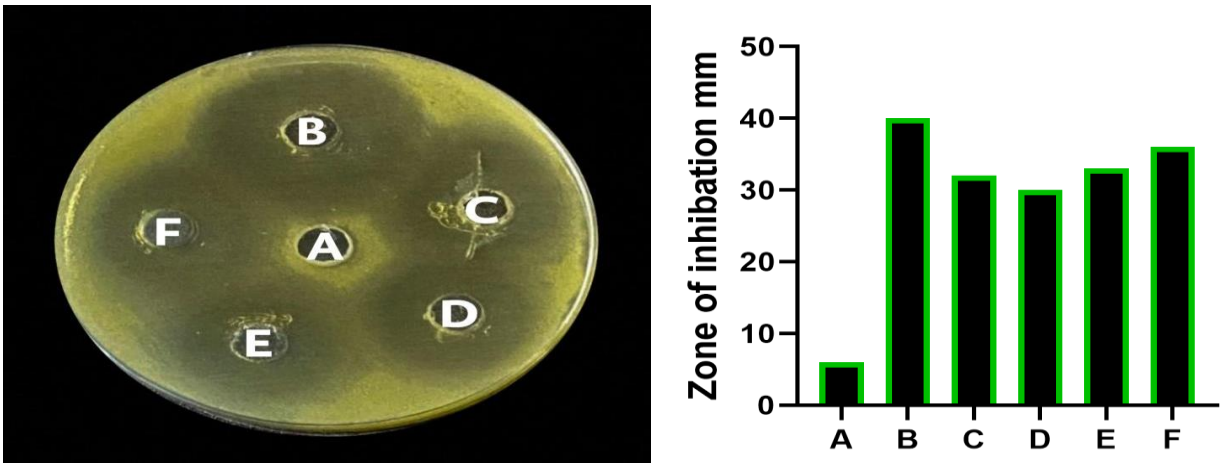

Figure 13: Streptococcus A, the control, was susceptible to H5 antibacterial effects. B: Levofloxacin 250 g/ml-treated bacterial strain. bacterium strain C, 50 g/ml treatment. 100 micrograms/ml were used to treat the D bacterial strain. 200 micrograms/ml were used to treat the bacterial strain E. bacterium strain F, 400 g/ml treatment.

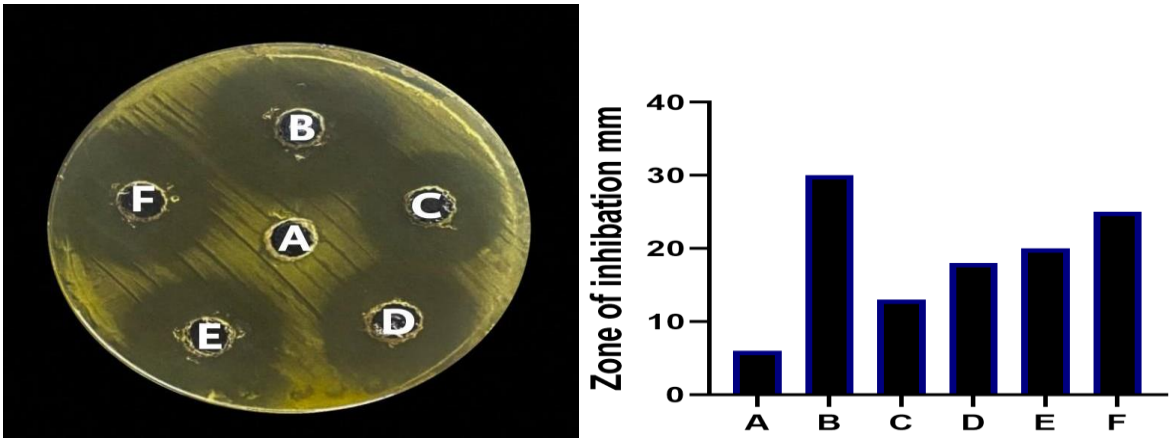

Figure 14: H5 antibacterial action on pseudomonas. A, instruction. Levofloxacin 250 micrograms/ml was used to treat the bacterial strain B. C, bacterial strain given a 50 microgram/ml treatment. D, bacterial strain given a 100 microgram/ml treatment. E, a bacterial strain that received 200 g/ml of treatment. F, 400 microgram/ml-treated strain of bacteria

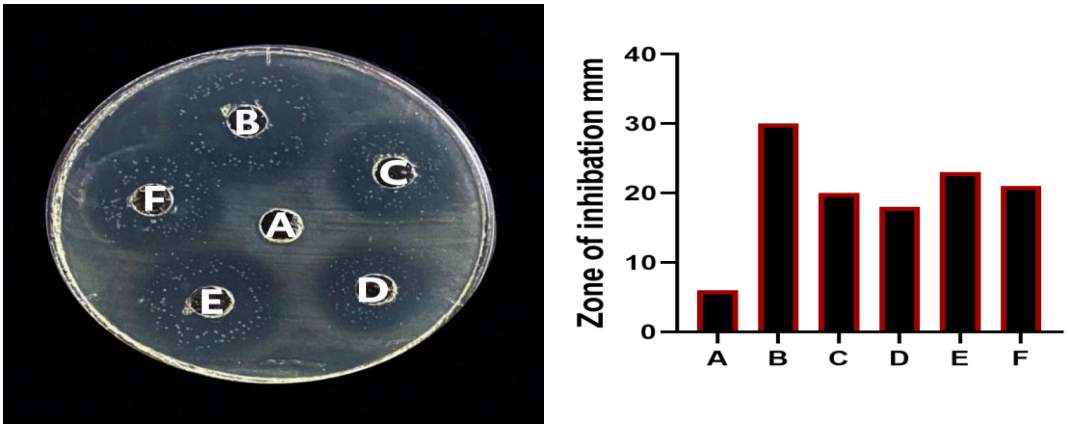

Figure 15: H5 antibacterial ability to combat Staphylococcus bacteria. A, command. Levofloxacin 250 micrograms/ml was used to treat the bacterial strain B. C, bacterial strain given a 50 microgram/ml treatment. D, bacterial strain given a 100 microgram/ml treatment. E, a bacterial strain that received 200 g/ml of treatment. F, 400 microgram/ml-treated strain of bacteria.

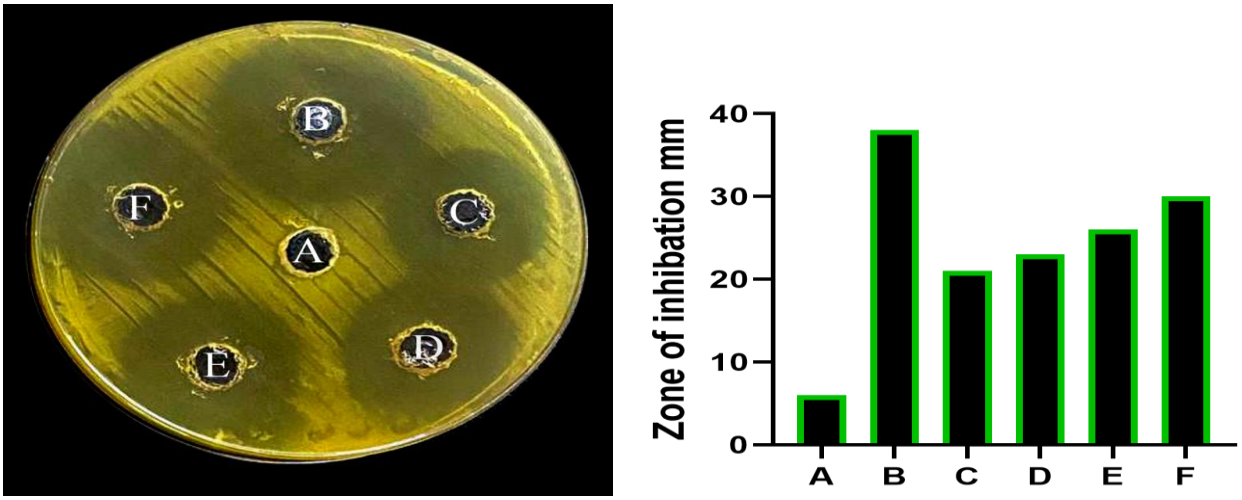

5. Conclusion:

After synthesizing two new derivatives of mono peptide H1, and dipeptide H5. Spectroscopic data were characterized as well as reactivity indices by using techniques FT-IR, ^{1}H-NMR, and ^{13}C-NMR. the bioactivity appeared studied for two levofloxacin derivatives compounds H1 and H5 have excellent results against three types bacteria of gram-positive and gram-negative bacteria.

References:

Sanders, L. M. Drug delivery system and routes of administration of peptide and protein drugs. Eur. J. Drug Metab. Pharmacokinet. 15, 95-102(1990).

Wang, G. Human antimicrobial peptides and proteins. Pharmaceuticals. 7(5). 545-594 (2014).

Bartlomiej, D. Marta, D. New milk protein-derived peptides with potential antimicrobial activity: An approach based on bioinformatic studies. Int. J. Mol. Sci. 15: 14531-14545 (2014).

World Health Organization, Antimicrobial resistance: global report on surveillance, 2014.

Chen L, Flies DB. Molecular mechanisms of T cell co-stimulation and co-inhibition. Nat. Rev. Immunol. 2013;13(4):227–242.

Wender, P.A. Cooley, C.B. Geihe, E.I. Beyond cell penetrating peptides: designed molecular transporters, Drug Discov. Today Technol. 9, e49–e55(2012).

Hyman, J.M. Geihe, E.I. Trantow, B.M. Parvin, B. Wender, P.A. A molecular method for the delivery of small molecules and proteins across the cell wall of algae using molecular transporters, Proc. Natl. Acad. Sci. U. S. A. 109, 13225–13230(2012).

Cheng, H. Zhu, J.Y. Xu, X.D. Qiu, W.X. Lei, Q. Han, K. Cheng, Y.J. Zhang, X.Z. Activable cell-penetrating peptide conjugated prodrug for tumor targeted drug delivery. ACS Appl. Mater. Interfaces 7 16061–16069(2015).

Iwata, Y. Akamatsu, H. Hasegawa, S. Takahashi, M. Yagami, A. Nakata, S. et al. The epidermal Integrin beta-1 and p75NTR positive cells proliferating and migrating during wound healing produce various growth factors, while the expression of p75NTR is decreased in patients with chronic skin ulcers. J. Dermat. Sci. 71, 122–129(2013).

Sathish JG, Sethu S, Bielsky MC, et al. Challenges and approaches for the development of safer immunomodulatory biologics. Nat. Rev. Drug Discov. 2013;12(4):306–324.

Aakanksha Rani, De Leon-Rodriguez, L. M. Iman K. Duncan J.M. David E.W. Margaret A.B. Synthesis and characterization of mono S-lipidated peptide hydrogels: a platform for the preparation of reactive oxygen species responsive materials, Org. Biomol. Chem.19, 3665–3677, 366596(2021).

Jayatunga MK, Thompson S, Hamilton AD. Alpha-helix mimetics: outwards and upwards. Bioorg. Med. Chem. Lett. 2014;24(3):717–724.

Dominici,M. Le Blanc, K. Mueller, I. Slaper-Cortenbach, I. Marini, F. C. Krause, D. S. et al. Minimal criteria for defining multipotent mesenchymal stromal cells. The InternationalSociety for Cellular Therapy position statement. Cytotherapy 8, 315–317(2006).

Ejiri, H. Nomura, T. Hasegawa, M. Tatsumi, C. Imai, M. Sakakibara, S. et al. Use of synthetic serum-free medium for culture of human dermal fibroblasts to establish an experimental system similar to living dermis. Cytotechnology 67, 507–514(2015).

Ge,W. Cheng, S.-F. Dyce, P.W. De Felici,M. and Sgen,W. Skin-derived stem cells as a source of primordial germ cell- and oocyte-like cells. Cell Death Dis. 7:e2471(2016).

Suresh Kumar Sharma, Gurpreet Singh, Ramesh Kataria, Harsh Kumar, Sanjay Sharma, Investigations on molecular interaction of some amino acids with the drug levofloxacin in aqueous solution by

volumetric and acoustic methods at different temperatures, J. Chem. Thermodynamics, S0021-9614(16)30286-5.

Golebiewska, E. M. and Poole, A. W. Platelet secretion: from haemostasis to wound healing and beyond. Blood Rev. 29, 153–162(2015).

Jabło´nska-Trypu´c, A. Matejczyk, M. and Rosochacki, S. Matrix metalloproteinases (MMPs), the main extracellular matrix (ECM) enzymes in collagen degradation, as a target for anticancer drugs. J. Enzyme Inhib. Med. Chem. 31, 177–183(2016).

Jansen, K. A. Atherton, O. and Ballestrem, C. Mechanotransduction at the cell-matrix interface. Semin. Cell Dev. Biol. 71, 75–83(2017).

Gokhale A, Kanthala S, Latendresse J, Taneja V, Satyanarayanajois S. Immunosuppression by co-stimulatory molecules: inhibition of CD2-CD48/CD58 interaction by peptides from CD2 to suppress progression of collagen-induced arthritis in mice. Chem. Biol. Drug Design. 2013;82(1):106–118.

Nam EJ, Kang JH, Sung S, et al. A matrix metalloproteinase 1-cleavable composite peptide derived from transforming growth factor beta-inducible gene h3 potently inhibits collagen-induced arthritis. Arthritis Rheum. 2013;65(7):1753–1763.

Jimi, S. Sato, K. Kimura, M. Suzumiya, J. Hara, S. Francesco, D. F. et al. G-CSF administration accelerates cutaneous wound healing accompanied with increased Pro-Hyp production in db/db mice. Clin. Res. Dermatol. 4, 1–9(2017)..

Shriner, R. I. and Hermann, C. K. " Spectroscopic Techniques for Organic Chemistry ". John Wiley and Sons , N. Y , 2004.

Martin, G. E. " Cryogenic NMR Probs: Application, Grant, D. M. and Harris, R. K. " Encyclopedia of Nuclear Magnetic Resonance. 9, Wiley Chichester, (2002).

Jimeno, M.L. Jagerovic, N. Elguero, J. Junk, T. Catallo, W.J. 1H and 13C NMR study of perdeuterated pyrazoles. Spectroscopy.13, 291–294(1997).

Lever, A. B.P. " Inorganic Electronic Spectroscopy ", 2nd Ed. Elsevier Science , (1984).

Kiehlbauch, J.A. et al. Use of the national committee for clinical laboratory standards (NCCLS) guidelines for disk diffusion susceptibility testing in New York state laboratories. J. Clin. Microbiol. 38, 3341–3348(2000).

Bahjat, H. H. Ismail, R.A. Sulaiman, G. M. and Jabir, M. S.. Magnetic field-assisted laser ablation of titanium dioxide nanoparticles in water for antibacterial applications. Journal of Inorganic and Organometallic Polymers and Materials, 1-8(2021).

Khashan, K.S. Abdulameer, F.A. Jabir, M.S. Hadi, A.A. and Sulaiman, G.M. Anticancer activity and toxicity of carbon nanoparticles produced by pulsed laser ablation of graphite in water. Advances in Natural Sciences: Nanoscience and Nanotechnology, 11(3), 035010(2020).

Khashan, K.S. Badr, B.A. Sulaiman, G.M. Jabir, M. S. and Hussain, S. A. Antibacterial activity of Zinc Oxide nanostructured materials synthesis by laser ablation method. In Journal of Physics: Conference Series. 1795(1), 012040(2021, March).

Jihad, M.A. Noori, F. Jabir, M. S. Albukhaty, S. AlMalki, F. A. and Alyamani, A.A. Polyethylene Glycol Functionalized Graphene Oxide Nanoparticles Loaded

with Nigella sativa Extract: A Smart Antibacterial Therapeutic Drug Delivery System. Molecules, 26(11), 3067(2021).

Mohammed, M.K. Mohammad, M.R. Jabir, M.S. and Ahmed, D.S. Functionalisation, characterisation, and antibacterial activity of single wall and multi wall carbon nanotubes. Conference Series: Materials Science and Engineering. 757(1), 012028(2020, March).

Ali, I.H. Jabir, M.S. Al-Shmgani, H.S. Sulaiman, G.M. and Sadoon, A.H. Pathological And immunological study on infection with escherichia coli in ale balb/c mice. In Journal of Physics: Conference Series. 1003(1), 012009 (2018, May). 170-

34- Younus, A. Al-Ahmer, S. and Jabir, M. Evaluation of some immunological markers in children with bacterial meningitis caused by Streptococcus pneumoniae. Research Journal of Biotechnology, 14, 131-133(2019).